

LETTER TO THE EDITOR

Detection of circumstellar nitric oxide Enhanced nitrogen abundance in IRC +10420^{*,**}

G. Quintana-Lacaci^{1,2}, M. Agúndez^{3,4}, J. Cernicharo¹, V. Bujarrabal⁵, C. Sánchez Contreras⁶,
A. Castro-Carrizo⁷, and J. Alcolea⁸

¹ Centro de Astrobiología (CSIC-INTA), Ctra de Torrejón a Ajalvir, km 4, 28850 Torrejón de Ardoz, Madrid, Spain
e-mail: [guillermoq;jose.cernicharo]@cab.inta-csic.es

² Instituto de Radio Astronomía Milimétrica (IRAM), Avenida Divina Pastora, núcleo central, 18012 Granada, Spain

³ Univ. Bordeaux, LAB, UMR 5804, 33270 Floirac, France

⁴ CNRS, LAB, UMR 5804, 33270 Floirac, France

e-mail: Marcelino.Agundez@obs.u-bordeaux1.fr

⁵ Observatorio Astronómico Nacional (IGN), Ap 112, 28803 Alcalá de Henares, Spain

e-mail: v.bujarrabal@oan.es

⁶ Centro de Astrobiología (CSIC-INTA), ESAC Campus, 28691 Villanueva de la Cañada, Madrid, Spain

e-mail: csanchez@cab.inta-csic.es

⁷ Institut de RadioAstronomie Millimétrique, 300 rue de la Piscine, 38406 Saint-Martin d'Hères, France

e-mail: ccarrizo@iram.fr

⁸ Observatorio Astronómico Nacional (IGN), Alfonso XII N3, 28014 Madrid, Spain

e-mail: j.alcolea@oan.es

Received 22 September 2013 / Accepted 29 October 2013

ABSTRACT

Aims. During a full line survey towards IRC +10420 in the 3 and 1 mm bands, we detected the emission of circumstellar nitric oxide for the first time. We aim to study the formation of NO and to confirm the enrichment of nitrogen expected for the most massive, evolved stars predicted by the hot bottom burning process.

Methods. We counted on a detailed model of the structure and kinematics of the molecular gas around IRC+10420. In addition, we used a chemical model to derive the NO abundance profile. We modified the initial nitrogen abundance in order to fit the observed NO profiles. These synthetic profiles were obtained using an LVG radiative transfer code.

Results. We have detected NO in a circumstellar envelope for the first time, along with a variety of N-rich molecules, which in turn shows that IRC +10420 presents a N-rich chemistry. Furthermore, we have found that to reproduce the observed NO line profiles, the initial abundance of nitrogen in the chemical model has to be increased by a factor 20 with respect to the values of the standard O-rich stars.

Key words. astrochemistry – line: identification – molecular processes – circumstellar matter – supergiants – stars: individual: IRC +10420

1. Introduction

IRC +10420 is one of the most massive and luminous stars known ($L \sim 5 \times 10^5 L_{\odot}$, $M_{\text{init}} \sim 50 M_{\odot}$; Tiffany et al. 2010; Nieuwenhuijzen & de Jager 2000). Despite its being located at 5 kpc from us (Jones et al. 1993), it is the yellow hypergiant star that has been studied the most.

The yellow hypergiants (YHGs) are post-red supergiant stars (RSGs) evolving blueward in the Hertzsprung-Russell diagram. The mass ejection in these objects is very effective. In fact, these stars are thought to lose as much as one half of their initial masses during the RSG phase (e.g., Maeder & Meynet 1988). In addition, during this evolution YHGs encounter an instability region called the yellow void (de Jager 1998), which results in new

episodes of effective mass ejection. However, only two YHGs have shown molecular emission, IRC+ 10420 and AFGL 2343.

The CO emission from these two objects has been carefully modelled by (Castro-Carrizo et al. 2007) using radiative transfer codes. These authors found that the molecular gas around these objects is mainly distributed spherically, showing an isotropical mass ejection with important radial gradients. In particular, for IRC+ 10420 they found two detached circumstellar envelopes (CSEs) with a maximum extent of 5×10^{17} cm expanding at high velocities ($\sim 37 \text{ km s}^{-1}$). These envelopes were formed during two strong mass ejections separated in time (1200 years between the ejections), reaching a mass loss rate of $3 \times 10^{-4} M_{\odot} \text{ yr}^{-1}$. The mass derived for the CSE around this object is $\sim 1 M_{\odot}$. Castro-Carrizo et al. (2001) found a detached shell of thermal SiO emission around IRC +10420. This SiO emission is located at 10^{17} cm from the star, far from the dust-formation region where SiO is usually located (Lucas et al. 1992). They suggest that this SiO emission is due to a shock front that would lead to the release of fresh SiO from the dust grains.

* Based on observations carried out with the IRAM 30 m Telescope. IRAM is supported by INSU/CNRS (France), MPG (Germany), and IGN (Spain).

** Figures 3 and 4 are available in electronic form at <http://www.aanda.org>

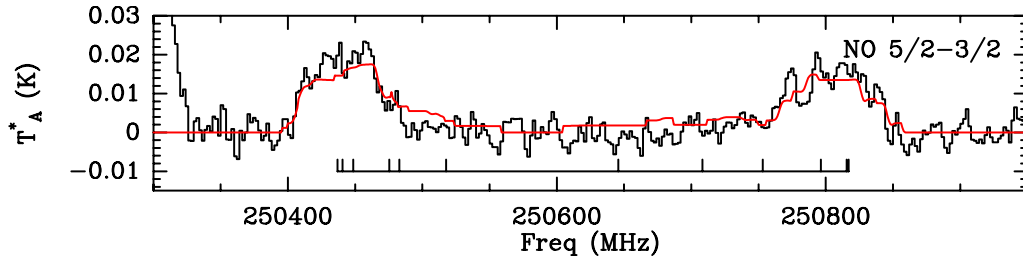


Fig. 1. Profiles of NO $J = 5/2-3/3$ detected towards IRC +10420. The hyperfine components of NO Π^+ and Π^- transitions cannot be resolved because of the high expansion velocity of this object. The different hyperfine transitions of each specie are represented by the ticks in the line below the profile. The red line shows the result of the model fitting described in Sect. 5.

Quintana-Lacaci (2008) showed that the molecular material observed by Castro-Carrizo et al. (2007) was only ejected during the YHG phase. No molecular gas expelled from the RSG phase was detected. This gas was rapidly diluted thanks to the high expansion velocities typical of these massive stars.

Quintana-Lacaci et al. (2007) found that the chemistry of IRC +10420 is particularly rich. The following species were detected in the CSE around this object: HCN, CN, H^{13}CN , SiO, ^{29}SiO , SO, SiS, HCO^+ , CN, HNC, and CS. Surprisingly, some species such as HCN and HNC show particularly high abundances compared to O-rich asymptotic giant branch (AGB) stars, which are the low-mass counterpart of YHGs. This could be explained by an enrichment in nitrogen due to the hot-bottom-burning process (Boothroyd et al. 1993), which is thought to operate in stars with masses above $\sim 3 M_{\odot}$. This process transforms ^{12}C into nitrogen, thereby changing the composition of the material that is transported to the photosphere of the star and expelled later on. For the most massive and evolved stars, the nitrogen enrichment is expected to lead to a N-rich chemistry.

Recently, Teyssier et al. (2012) have observed selected transitions of NH_3 , OH, H_2O , CO, and ^{13}CO with HIFI towards this object. They also show that the model derived by Castro-Carrizo et al. (2007) for low- J CO transitions was applicable, with minor changes, to higher excitation lines.

Although several N-bearing molecules have been detected, none of them contain oxygen, which is the most abundant atom after H and He in YHGs. In this Letter we present the first detection of nitric oxide in a CSE.

2. Observations

We used the IRAM 30 m radiotelescope to perform a complete line survey in the 3 mm and 1 mm bands towards the YHG IRC +10420 (Quintana-Lacaci et al., in prep.). IRC +10420 was observed at the position coordinates (J2000) $19^{\text{h}}26^{\text{m}}48^{\text{s}}.10$, $+11^{\circ}21'17''.0$, with an $V_{\text{LSR}} = 76 \text{ km s}^{-1}$. We used the EMIR receiver, using simultaneously the receivers E090 and E230, with a bandwidth of 4 GHz at two polarizations. We used 16 different frequency setups to cover the atmospheric windows at 3 mm and 1 mm. Each setup was observed for one hour. We observed using the wobbler switching mode. The system temperatures were 100–250 K for the E090 receiver and between 200 and 425 K for the E230 receiver. During the observations, the amount of precipitable water vapour ranged between 2 and 6 mm.

The backends used were WILMA (spectral resolution 2 MHz) and the 4 MHz filter bank. Due to the large width ($\sim 60 \text{ km s}^{-1}$) of the line profiles of the lines observed in IRC +10420, this resolution is enough to resolve line profiles. The typical rms obtained for the observations ranged

between 0.8 and 1.5 mK at 3 mm and between 2.0 and 2.7 mK at 1 mm.

The pointing correction was checked frequently, and, therefore we expect pointing errors of $\sim 3''$. The spatial resolution at 3 mm is $21-29''$ and $9-13''$ at 1 mm. The data presented here are calibrated in antenna temperature (T_{A}^*). The calibration error is expected to be 20%. The data were processed using the GILDAS package¹. The baselines were subtracted using only first grade polynomials.

3. Detection of NO

A first result of the line survey described above is the first detection of NO around an evolved star (see Fig. 1). The whole survey will be presented in a forthcoming paper (Quintana-Lacaci et al. in prep.). Recently, NO emission has also been detected towards the O-rich PPN OH231.8 (Sánchez Contreras et al., priv. comm.). This is the only NO transition covered by the line survey mentioned above.

The NO transition detected consisted in the two Π bands of the transition $J = 5/2-3/2$. The integrated intensity of the NO $J = 5/2-3/2$ transitions is 2.99 K km s^{-1} , being in particular 1.59 K km s^{-1} for the Π^+ band and 1.40 for the Π^- band. The temperature scale is T_{A}^* .

Quintana-Lacaci et al. (2007) showed that the rotational temperature derived for the different molecules in IRC +10420 may vary from 6 K for CN to 36 for HCN, or 79 K for SiO. This shows that in order to reasonably determine the abundance of the different molecules in this envelope at least we need two transitions. New observations of NO transitions are fundamental to be able to study the characteristics of this emission in a proper way.

These authors restricted the emission of all molecular lines, but those of CO, to a region with a diameter of $3''.3$. Since the HPBW at the relevant frequencies is $\sim 9''$, the line emission of NO is expected to be well covered by the beam of the telescope. Assuming this extent for the emission, the mean rotational temperature, $T_{\text{rot}} = 11 \text{ K}$, obtained by Quintana-Lacaci et al. (2007), and an LTE excitation, we obtain a column density of NO of $2.5 \times 10^{16} \text{ cm}^{-2}$, which corresponds to an abundance relative to H_2 of $\sim 4 \pm_{-3}^{+1} \times 10^{-5}$. We found that this abundance is particularly high compared with the abundances derived for the other molecules detected in the line survey, assuming the same LTE and temperature assumptions as for NO (Quintana-Lacaci et al., in prep.). This is confirmed by the results by Quintana-Lacaci et al. (2007). In particular, only the abundance of ^{12}CO is higher than that of NO, being on the other hand that of ^{13}CO similar to it.

In addition to NO, we have detected a large number of N-rich molecules toward IRC +10420, as a result of the expected

¹ See URL <http://www.iram.fr/IRAMFR/GILDAS/>

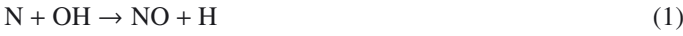
Table 1. Parameters of the molecular emission model by [Teyssier et al. \(2012\)](#).

Shell	R_{in} (cm)	R_{out} (cm)	$\dot{M}(M_{\odot} \text{ yr}^{-1})$	T_{17} (K)	α_t	V_{exp} (km s $^{-1}$)	σ_{turb} (km s $^{-1}$)
1	2.5×10^{16}	1.24×10^{17}	3×10^{-4}	170	1.2	37	3
2	2.2×10^{17}	5.2×10^{17}	1.2×10^{-4}	100	0.8	25	20

nitrogen enrichment due to the hot bottom burning. As a summary, all the N-rich species found in this object are NO, NS, PN, N_2H^+ , NH_3 , HCN, HNC, H^{13}CN , and CN (see Figs. 3 and 4 for the lines detected in the line survey mentioned above). This proves that IRC +10420 presents N-rich chemistry. The analysis of the data for those molecules is in progress and will be published elsewhere.

4. Formation of NO in O-rich CSEs

The chemistry of nitric oxide in the cold interstellar medium (see [Gerin et al. 1992](#); [Hily-Blant et al. 2010](#)) is controlled by the gas phase reactions,



and



which are barrierless ([Daranlot et al. 2011](#); [Bergeat et al. 2009](#)) and therefore rapid at the low temperatures of interstellar clouds. NO is formed from nitrogen atoms and hydroxyl radicals through reaction (1) and becomes a major intermediate in the synthesis of N_2 through reaction (2). Many of the chemical reactions that synthesize molecules in interstellar clouds are also at work in CSEs around evolved stars, although one major difference in the chemistry of these two environments concerns the chemical composition of the starting bulk material, which in CSEs is given to a large extent by thermochemical equilibrium at the temperatures and pressures characteristic of the surroundings of the star.

To gain insight into the synthesis of nitric oxide in IRC +10420, we carried out a chemical model based on the physical structure presented by [Teyssier et al. \(2012\)](#), which reproduces the observations for low and high CO excitation lines. The mass-loss history derived for this object consisted of two mass ejection episodes from the star, which resulted in two detached shells (see Table 1). This gas is expelled at very high velocities ($\sim 37 \text{ km s}^{-1}$), which are directly related to the high luminosity of the central star.

In a similar way to [Quintana-Lacaci et al. \(2007\)](#), we assumed that the emission from the molecular species different from CO is restricted only to the inner shell. At the large distances from the star that define the outer shell (2.2×10^{17} – 5.2×10^{17} cm), the density of the gas is very low, and only species with high abundances and strong self-shielding would avoid photodissociation, in particular CO.

In summary, the chemical model considers an oxygen-rich CSE that expands spherically with the mass loss rate, expansion velocity, radial temperature profile, and initial radius of shell 1 of IRC +10420 (see Table 1). The chemical model is similar to those presented previously for carbon-rich CSEs (e.g., [Agúndez et al. 2008](#)), although in this case we consider molecular abundances at the initial radius typical of the inner regions of O-rich CSEs, which come from observations or from thermochemical equilibrium calculations (see values and references in [Agúndez 2009](#)). In the specific case of nitrogen, we consider that at the

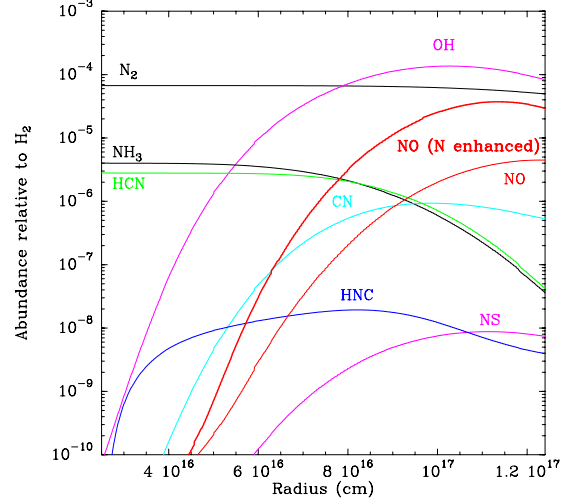


Fig. 2. Calculated abundances of some N-bearing molecules as a function of radius for an O-rich CSE (see text). The abundance profile of NO needed to fit the data, result of an N-enhancement, is shown with a thick red line.

inner radius this element is mostly in the form of N_2 , with an abundance relative to H_2 of 6.75×10^{-5} (based on the solar elemental abundance of nitrogen). NH_3 and HCN are also taken into account in our model with somewhat lower abundances relative to H_2 of 4×10^{-6} and 2.8×10^{-6} , respectively ([Menten & Alcolea 1995](#); [Quintana-Lacaci et al. in prep.](#)). As the gas expands from the initial radius, molecules start to be exposed to the ambient interstellar ultraviolet field, and photochemistry drives the formation of new species. Figure 2 shows the resulting abundances of some nitrogen-bearing molecules as a function of radius. It is seen that, for a standard O-rich AGB star, nitric oxide is formed with a maximum abundance relative to H_2 of $\sim 4 \times 10^{-6}$. Similar to the case of the interstellar medium, the main formation route of NO involves reaction (1), although in this case the nitrogen atoms and hydroxyl radicals come from the photodissociation of the parent molecules N_2 and H_2O , respectively, and NO is destroyed mainly by photodissociation. Therefore, the chemical model predicts that nitric oxide forms by photochemistry in the outer circumstellar layers, where it becomes the major nitrogen-bearing molecule. For the chemical model, we assume an abundance of 3×10^{-4} for H_2O ([Maercker et al. 2008](#)). Our results concerning NO agree with previous chemical models of O-rich CSEs ([Nejad & Millar 1988](#)). In view of its large predicted abundance, it seems that its low dipole moment has so far prevented the detection of this molecule in an oxygen-rich CSE.

5. Modelling the NO emission

To model the observed NO line profiles and to calculate the excitation of the transitions involved, we have used the molecular emission model of IRC +10420 by [Teyssier et al. \(2012\)](#) restricted to the inner shell, using as radial abundance profile for NO that computed with the chemical model. As mentioned above, this model reproduces the characteristics of the molecular gas at high and low excitation regimes. In addition, our chemical

model predicts that NO cannot reach the second shell. This supports our assumption for the size of the NO emitting region. Therefore, we expect the values derived below for the NO abundance and the N/O and N/H ratios to be good approximation to the reality.

We used the radiative transfer code MADEX (Cernicharo 2012) to solve the level population at the different radii of the envelope. The line excitation and the population of the rotational levels were calculated using the LVG approximation; i.e., we assumed that the velocity gradient in the envelope of the star is such that the gas at the different radii is radiatively isolated. The radiative transfer equations are then solved and the resulting brightness distribution is convolved with the beam of the telescope. This results in synthetic spectra that can be directly compared with the observations.

MADEX assumes spherical symmetry. This assumption is reasonable in this case since, while the outer shell of IRC +10420 shows a departure from the spherical symmetry, the inner shell is mainly spherical (Castro-Carrizo et al. 2001, 2007).

The line intensities of NO obtained using abundance profile described above were very weak compared with the observations (by around a factor 20). Since, as mentioned, we expect this object to be similar to O-rich evolved stars, but showing a particularly high abundance of nitrogen, we increased the abundance of nitrogen at the initial radius to obtain a new abundance profile of NO that fits the observed data. We increased the nitrogen abundance by a factor 20 to obtain the best fit. This enhancement in the N₂ abundance results in an increase in the peak abundance of NO of about a factor 10. We estimate that the error of this enhancement is at least of a factor 2 when considering that we do not know the exact size of the emitting region and that infrared pumping that could affect the population of the NO rotational levels has not been taken into account (Daniel et al. 2012). This enhancement results in very significant lower limits for the abundance ratios: N/H $\geq 7 \times 10^{-4}$ and N/O ≥ 2 .

An enrichment in nitrogen due to the HBB would result at the same time in a decrease in the amount of carbon available to form C-bearing molecules. Therefore, less nitrogen would be used to form molecules containing carbon and nitrogen as HCN, and more nitrogen would be available to form molecules as NH₃ and NO. We checked the result of our chemical model assuming that carbon is only located in CO; i.e., HCN and CO₂ are not formed, and find that the NO abundance is not sensitive to these changes. As mentioned above, the NO abundance is directly related to the abundance of N₂ and H₂O and to the assumptions of the chemical model, i.e. the photodissociation of the N₂. If N₂ is photodissociated faster than assumed in our chemical model (Bohlin et al. 1978) the enhancement of nitrogen needed to fit the NO profiles would not be that high. Also, a detailed modeling of the line emission from H₂O presented by Teyssier et al. (2012) would help check that the abundance of this molecule is higher than what is assumed in the present work, which would result in lower nitrogen abundances. The model fitting is shown in Fig. 1, while in Fig. 2 we compare the abundance profile obtained for a standard O-rich evolved star, in which a solar nitrogen budget is considered, and what is needed to fit the NO lines observed in IRC +10420. In particular, the maximum NO abundance reached for an O-rich star is expected to be $\sim 4 \times 10^{-6}$, while the abundance needed to reproduce the observed NO spectra is $\sim 4 \times 10^{-5}$. This high abundance coincides with the value derived assuming LTE in Sect. 3.

It is important to note that our fitting has been based in a single *J* transition. A detailed modeling of different *J* transitions of NO and of rotational transitions of the rest of the N-rich molecules observed would show the validity of the chemical model used in this work or impose constraint on the reactions involved. A paper devoted to a global fitting of the N-rich abundance profiles is in preparation.

6. Conclusions

We have detected circumstellar NO for the first time in the YHG IRC +10420. To reproduce the NO line profiles observed we had to increase the initial abundance of nitrogen in the chemical model, which confirms the N-enhancement predicted by the hot bottom burning process for massive stars. The values derived for the abundance ratios N/H and N/O are remarkably high. In particular, the lower limits for these ratios are N/H $\geq 7 \times 10^{-4}$ and N/O ≥ 2 .

The relative abundance found for NO in IRC +10420 reaches a maximum of 4×10^{-5} . This high abundance shows that NO is indeed the most abundant nitrogen-bearing molecule in the circumstellar gas of IRC +10420. The detection of this molecule has most likely been prevented so far thanks to its low dipole moment. In addition, in IRC +10420 we detected cyanides (HCN, HNC, CN), nitric hydrides (N₂H⁺, NH₃), and other N-bearing molecules, such as NS and PN. These detections confirm the N-rich chemistry expected as a result of the nitrogen enrichment found in IRC +10420.

Acknowledgements. We would like to thank the Spanish MINECO for funding support from grants CSD2009-00038, AYA2009-07304 & AYA2012-32032.

References

- Agúndez, M. 2009, Ph.D. Thesis, Universidad Autónoma de Madrid
 Agúndez, M., Fonfría, J. P., Cernicharo, J., Pardo, J. R., & Guélin, M. 2008, *A&A*, 479, 493
 Bergeat, A., Hickson, K. M., Daugey, N., Caubet, P., & Costes, M. 2009, *Phys. Chem. Chem. Phys. (Incorporating Faraday Transactions)*, 11, 8149
 Bohlin, R. C., Savage, B. D., & Drake, J. F. 1978, *ApJ*, 224, 132
 Boothroyd, A. I., Sackmann, I.-J., & Ahern, S. C. 1993, *ApJ*, 416, 762
 Castro-Carrizo, A., Lucas, R., Bujarrabal, V., Colomer, F., & Alcolea, J. 2001, *A&A*, 368, L34
 Castro-Carrizo, A., Quintana-Lacaci, G., Bujarrabal, V., Neri, R., & Alcolea, J. 2007, *A&A*, 465, 457
 Cernicharo, J. 2012, in *ECLA-2011: Proc. European Conference on Laboratory Astrophysics*, EAS PS, 58, 251
 Daniel, F., Agúndez, M., Cernicharo, J., et al. 2012, *A&A*, 542, A37
 Daranlot, J., Jorfi, M., Xie, C., et al. 2011, *Science*, 334, 1538
 de Jager, C. 1998, *A&ARv*, 8, 145
 Gerin, M., Viala, Y., Pauzat, F., & Ellinger, Y. 1992, *A&A*, 266, 463
 Hily-Blant, P., Walmsley, M., Pineau Des Forêts, G., & Flower, D. 2010, *A&A*, 513, A41
 Jones, T. J., Humphreys, R. M., Gehrz, R. D., et al. 1993, *ApJ*, 411, 323
 Lucas, R., Bujarrabal, V., Guilloteau, S., et al. 1992, *A&A*, 262, 491
 Maeder, A., & Meynet, G. 1988, *A&AS*, 76, 411
 Maercker, M., Schöier, F. L., Olofsson, H., Bergman, P., & Ramstedt, S. 2008, *A&A*, 479, 779
 Menten, K. M., & Alcolea, J. 1995, *ApJ*, 448, 416
 Nejad, L. A. M., & Millar, T. J. 1988, *MNRAS*, 230, 79
 Nieuwenhuijzen, H., & de Jager, C. 2000, *A&A*, 353, 163
 Quintana-Lacaci, G. 2008, Ph.D. Thesis, Universidad Autónoma de Madrid
 Quintana-Lacaci, G., Bujarrabal, V., Castro-Carrizo, A., & Alcolea, J. 2007, *A&A*, 471, 551
 Teyssier, D., Quintana-Lacaci, G., Marston, A. P., et al. 2012, *A&A*, 545, A99
 Tiffany, C., Humphreys, R. M., Jones, T. J., & Davidson, K. 2010, *AJ*, 140, 339

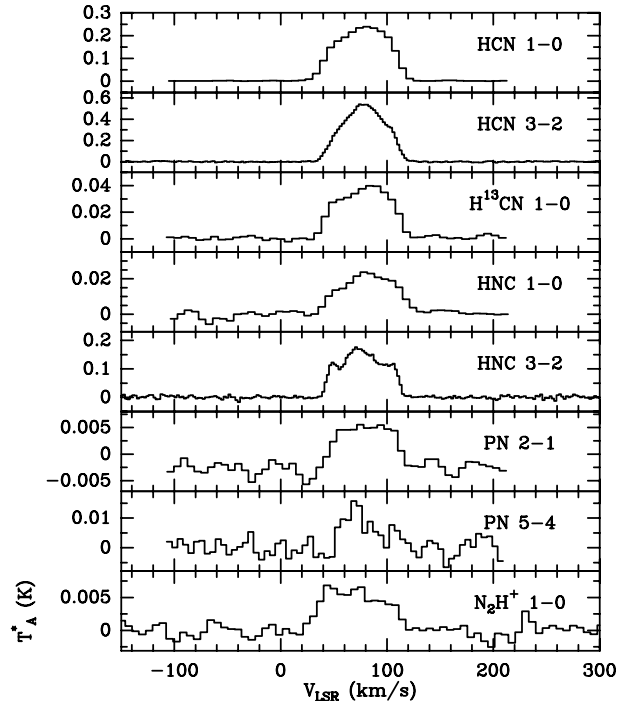


Fig. 3. Profiles of the N-rich species HCN, HNC, PN, N_2H^+ observed for IRC +10420.

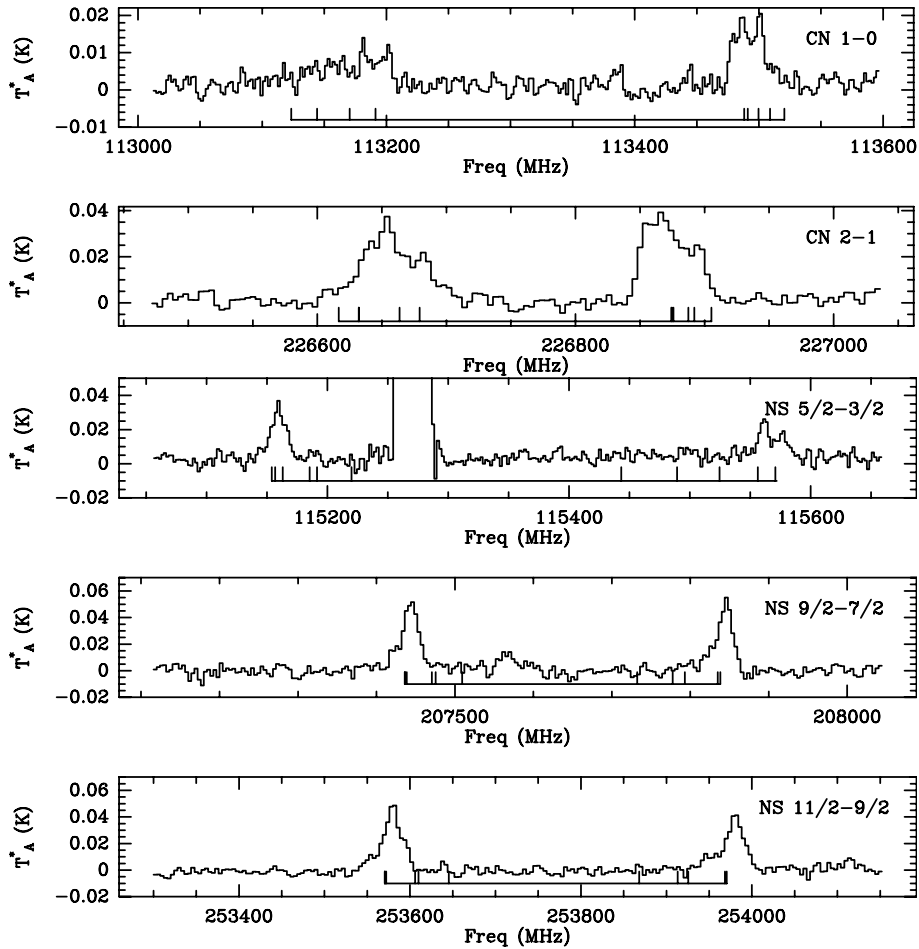


Fig. 4. Profiles of the N-rich species CN and NS observed for IRC +10420. The hyperfine components of these transitions cannot be resolved due to the high expansion velocity of this object. The different hyperfine transitions of each species are represented by the ticks in the line below the profile.